Photoperoxidation of a Diamino Zinc Porphyrazine to the *seco*-Zinc Porphyrazine: Suicide or Murder?

A. Garrido Montalban,[†] H. G. Meunier,[‡] R. B. Ostler,[†] A. G. M. Barrett,[†] B. M. Hoffman,[§] and G. Rumbles*,[†]

Department of Chemistry, Imperial College, London SW7 2AY, U.K., and Department of Chemistry, Northwestern University, Evanston, Illinois, 60208

Received: February 10, 1999

We report on the efficient photooxidation of hexapropyl bis(dimethylamino) zinc porphyrazine. The process is shown to be autocatalytic. The triplet state of the *seco*-ZnPz sensitizes the formation of excited-state singlet oxygen with a quantum yield of 0.54 and subsequent cleavage of the pyrrole double bond occurs to give the product, *seco*-zinc porphyrazine. The photophysics of the two porphyrazines is examined using absorption, emission, and transient absorption spectroscopy. The efficiency of production of singlet oxygen is monitored using the phosphorescence emission signature at 1270 nm.

Introduction

We reported recently the synthesis of porphyrazineoctamines by macrocyclization of diamino maleonitrile derivatives using magnesium propoxide in propanol.[1] During several Linstead macrocyclization[2] reactions of bis(dimethylamino)maleonitrile, we observed the formation of a minor side product, the *seco*-porphyrazine **1** (Figure 1).[3] In a subsequent article we reported a more general chemical oxidation strategy toward these new class of tetraazamacrocycles[4,5] where the zinc *seco*-porphyrazine (*seco*-ZnPz) **4** was obtained in high yield from the potassium permanganate-mediated oxidation of the zinc porphyrazine **2** (Figure 1) (ZnPz). Similar structural types have been reported recently by Dolphin and co-workers.[6] We noticed that slow oxidation also occurred when solutions of the zinc complex **2** and related analogues were left standing for prolonged times. The reaction was found to be efficient in chlorinated solvents (CH_2Cl_2, $CHCl_3$) but not in coordinating solvents such as pyridine and DMF. The reaction mechanism was rationalized in terms of a formal 2 + 2 cycloaddition of singlet oxygen to one of the activated pyrrol rings, followed by cleavage (retro 2 + 2) of the dioxetane intermediate **3** to produce zinc *seco*-porphyrazine **4**, as shown in Figure 1.

In this paper, we report the results from the photophysical studies of both the reactant, **2**, and product, **4**, and show that the full reaction mechanism of the photoperoxidation involves attack on the reactant by singlet oxygen that has been sensitized by the triplet state of the product. As a consequence, the kinetics of the process are shown to be autocatalytic where the reactant is removed at a rate that increases with the amount of product formed.

Experimental Section

Chemicals. The preparation, purification and characterization of ZnPz and *seco*-ZnPz have been described previously.[4] Solvents were purchased as GPR grade (BDH chemicals) and were found to be usable without further purification. Chlorophyll *a* (Aldrich Chemicals) was used without further purification.

Steady-State Absorption and Emission Measurements. Electronic absorption spectra were recorded on a dual beam UV/vis spectrometer (Perkin-Elmer Lambda-2) with fixed 2 nm resolution. Fluorescence emission and excitation spectra were recorded on a spectrometer with xenon arc lamp excitation and a photon-counting detection system (Instruments SA Fluoromax). Fluorescence quantum yields were determined by the comparative method[7] using chlorophyll *a* in ether ($\phi_F = 0.32 \pm 0.05$) as the reference standard. To avoid unwanted reabsorption effects, all fluorescence measurements were recorded on solutions with Q-band absorbances of less than 0.1 in 1 cm path length cells.

Time-Resolved Fluorescence Measurements. Fluorescence decays were recorded using a time-correlated single-photon counting spectrometer with pulsed laser excitation at an excitation wavelength, λ_{ex}, of 670 nm, 10 ps pulse duration, and a repetition rate of 3.8 MHz. Fluorescence was detected perpendicular to the direction of excitation, dispersed through a subtractive dispersion monochromator, and subsequently detected by a microchannel plate photomultiplier tube that provided an overall time resolution of less than 100 ps. The decays were analyzed using a nonlinear, least-squares, iterative reconvolution procedure and stringent data fitting criteria.[8]

Triplet State Measurements. Transient absorption spectra and singlet oxygen quantum yields were measured on a nanosecond, flash photolysis apparatus. Excitation light at 682 nm and a repetition rate of 10 Hz was provided by a tuneable pulsed dye laser that was pumped by the frequency doubled output of a Nd:YAG laser. A 75 W pulsed xenon lamp was used as the monitor source of white light and was detected through a monochromator using a photomultiplier tube connected to a computer-interfaced digital oscilloscope. Triplet state quantum yields were determined by the comparative technique[9] using chlorophyll *a* in ether as the reference standard ($\phi_T = 0.54 \pm 0.01$[10]).

* Corresponding author. E-mail: g.rumbles@imperial.ac.uk.
‡ Permanent address: Department of Chemistry, Assumption College, Worcester, MA 01609.
† Imperial College.
§ Northwestern University.

10.1021/jp9905068 CCC: $18.00
Published on Web 05/19/1999

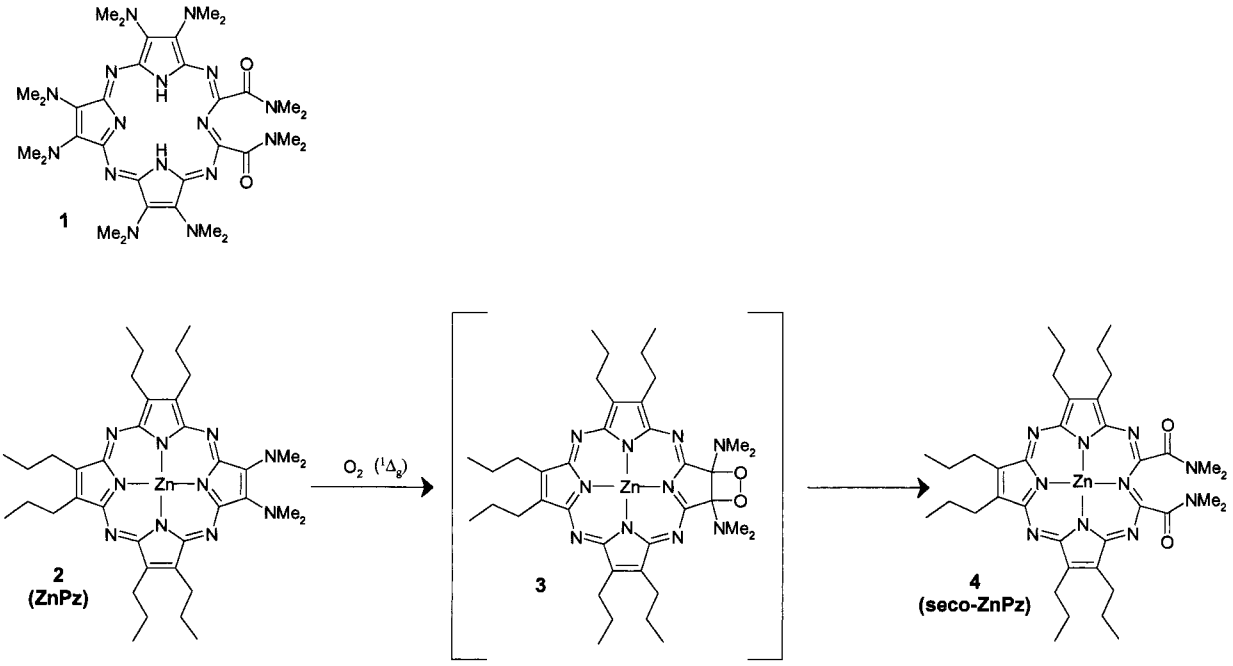

Figure 1. Mechanism for the synthesis of *seco*-zinc porphyrazine **4** (*seco*-ZnPz) by the attack of singlet oxygen on zinc porphyrazine **2** (ZnPz).

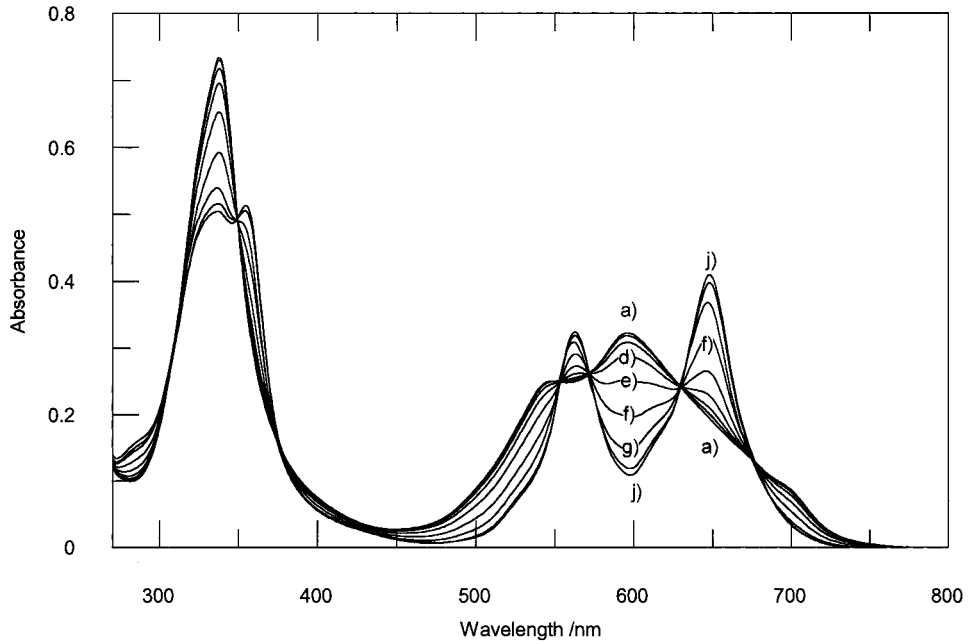

Figure 2. Absorption spectra of a sample of 1.07×10^{-5} M ZnPz in cyclohexane recorded after (a) 0; (b) 10; (c) 20; (d) 30; (e) 40; (f) 50; (g) 60; (h) 70; (j) >70 min irradiation time.

Singlet oxygen phosphorescence decays were detected at 1270 nm using a cooled germanium detector (North Coast). The quantum yield of singlet oxygen formation, ϕ_Δ, was calculated relative to chlorophyll *a* in the toluene as the reference sample ($\phi_\Delta = 0.6$[11]), with the effect of laser saturation eliminated by measuring the intensity of singlet oxygen phosphorescence as a function of laser power.

Results

The electronic absorption spectrum of ZnPz **2** has a distinct Q-band at 600 nm (see Figure 2a) which consists of two absorption features assigned to the nondegenerate and perpendicular Q_X and Q_Y transitions broadened by vibronic structure and the effect of the two amine groups. When the pyrrole bond is cleaved to form the *seco*-ZnPz **4**, the Q-band becomes two sharp peaks (see Figure 2j); the two carboxamine groups do not strongly interact with the central ring and the broadening effect is removed. A similar, but less pronounced, splitting can also be seen in the B, or Soret band at 350 nm. With these distinctive spectral changes the reaction can be readily followed using UV/vis electronic spectroscopy.

A purified sample of ZnPz was dissolved in cyclohexane to a concentration of 1.07×10^{-5} mol dm^{-3}, placed in a conventional 1 cm cuvette, and allowed to equilibrate with air at 295 K and an absorption spectrum was measured. The sample was irradiated with white light by placing it 30 cm in front of a 60 W tungsten filament lamp for 10 min. The sample was then returned to the spectrometer and a new spectrum was

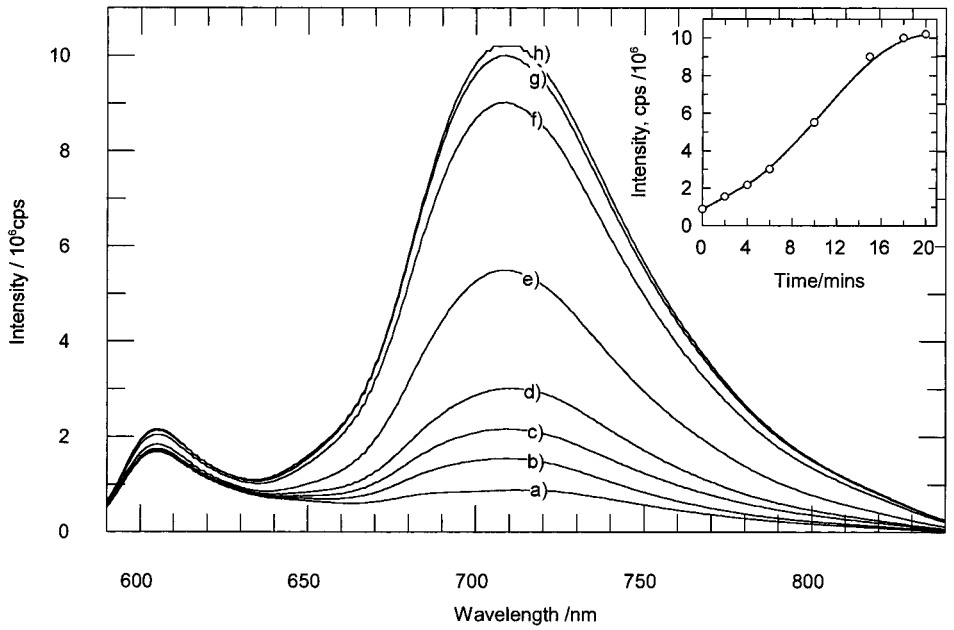

Figure 3. Fluorescence emission spectra (uncorrected) of a sample of 1.07×10^{-5} M ZnPz in cyclohexane recorded after (a) 0; (b) 2; (c) 4; (d) 6; (e) 10; (f) 15; (g) 18; (h) >18 min irradiation time. Excitation wavelength $\lambda_{ex} = 576$ nm. The inset shows the intensity at 708 nm as a function of time.

recorded. This process was then repeated until no further changes in the spectrum could be observed. The results from this study are shown in Figure 2.

The same process was repeated and monitored using fluorescence spectroscopy by exciting at 574 nm, a wavelength that corresponds to an isosbestic point in the absorption profiles in Figure 2. The results are shown in Figure 3.

Before irradiation the emission shows one peak at 605 nm. A new peak at 708 nm grows in with irradiation, reaching a maximum after 20 min, as shown in the inset of Figure 3. The fluorescence quantum yield of the emission at long times was determined to be 3.5×10^{-3}, a value which can be assigned to the *seco*-ZnPz product. The emission at 605 nm is independent of irradiation time, with the small increase attributable to the overlap of the emission that is centered at 708 nm. As the intensity of this peak does not change with irradiation, it cannot arise from either the ZnPz or the *seco*-ZnPz and is assigned to a very small amount of residual octapropyl zinc porphyrazine, which has a fluorescence quantum yield that we have measured to be approximately 50%.

Fluorescence decays of *seco*-ZnPz at various emission wavelengths were measured after irradiation and were adequately described by a biexponential function with decay times of 0.73 ns and 0.16 ns and contributions of 76.6% and 23.4%, respectively. A fresh sample of ZnPz in degassed toluene was prepared in order to record fluorescence emission and excitation spectra of the ZnPz, but no fluorescence was detected, although the 605 nm peak attributed to the octapropyl zinc porphyrazine was still evident.

The fluorescence data for ZnPz and *seco*-ZnPz suggest that the major deactivation pathways for the excited state of each are nonradiative. The possibility that this is due to intersystem crossing to the triplet state was then investigated using kinetic and spectral transient absorption spectroscopy. Figure 4 shows the excited ground state difference spectrum of *seco*-ZnPz immediately after the flash.

Bleaching of the ground state population is clearly indicated by the depletion in the absorption cross section of the sample

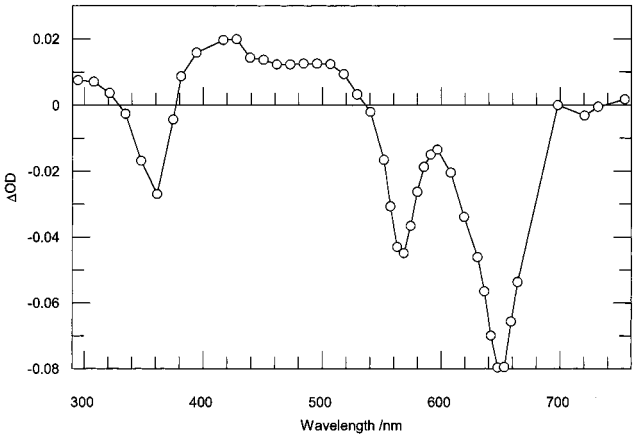

Figure 4. Transient absorption spectrum of *seco*-ZnPz sample. Excitation wavelength $\lambda_{ex} = 682$ nm.

at 650 and 560 nm, corresponding to the Q-bands, and at 340 nm, corresponding to the Soret band. To this bleaching is added a broad triplet state ($T_1 \rightarrow T_n$) absorption that is clearly observed in the region 390−520 nm, where little ground-state singlet ($S_0 \rightarrow S_n$) absorption occurs. The extinction coefficient at the maximum in this range, 427 nm, was calculated to be 0.97×10^4 dm^3 mol^{-1} cm^{-1} and the quantum yield for triplet state formation, ϕ_T, as 0.64 ± 0.06. A typical transient decay profile for air-free *seco*-ZnPz in this spectral region is shown in Figure 5 and is well described by an exponential function with a characteristic lifetime of 81 μs.

A sample of air-equilibrated *seco*-ZnPz in toluene solution was then investigated by observing the effect of the $^3O_2$ on the transient absorption decay and also by detecting emission at 1270 nm, where singlet oxygen phosphoresces. The change in the transient decay rate of the *seco*-ZnPz was so dramatic as to be difficult to measure accurately. Conversely, characteristic singlet oxygen emission was readily observed indicating that the triplet state of the *seco*-ZnPz was efficiently quenched by the dissolved oxygen. The singlet oxygen emission decayed exponentially with a characteristic lifetime of 29 μs, as shown

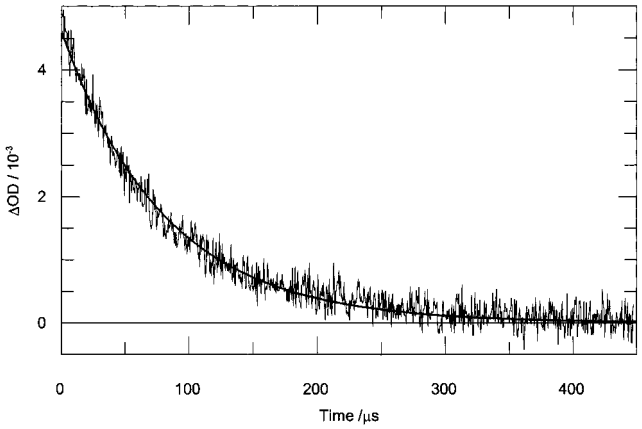

Figure 5. Transient decay profile of *seco*-ZnPz in toluene, recorded at 427 nm. Excitation wavelength, λ_{ex}, = 682 nm. The solid line is a fit to the function $A \exp(-t/\tau)$ where $A = 4.6 \times 10^{-3}$ and $\tau = 81.0$ μs.

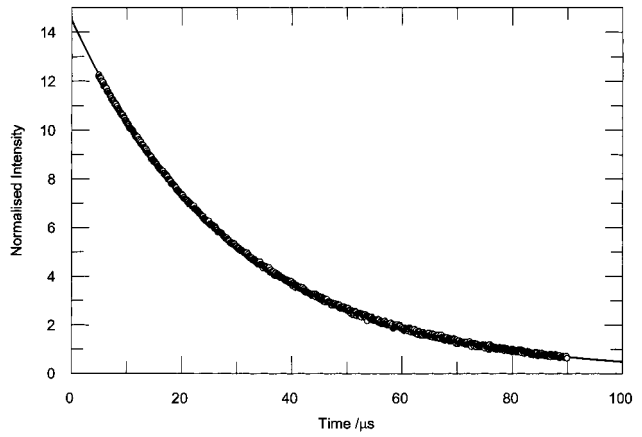

Figure 6. Decay of singlet oxygen emission at 1270 nm. The solid line is a fit to the function $A \exp(-t/\tau)$ where $A = 0.145$ and $\tau = 29.4$ μs.

in Figure 6, with no evidence of a grow-in component. The quantum yield of singlet oxygen formation sensitized by triplet *seco*-ZnPz, ϕ_Δ, was determined to be 0.54.

Attempts to record transient absorption data for the ZnPz failed to produce anything that could be assigned to a triplet absorption, although ground-state bleaching was still observed. Although no triplet states were detected, the sample was then air-equilibrated, and an attempt to observe emission from singlet oxygen was then made. This was an inherently difficult experiment as the light from the intense excitation flash was more than sufficient to promote the photoperoxidation reaction to form the *seco*-ZnPz. No singlet oxygen emission signal was detected initially, but a signal appeared rapidly and the intensity reached a maximum after only 10 s, which corresponds to 100 laser pulses. It was noted, however, that the emission decays within this short time frame did exhibit similar decay profiles. Absorption spectra of the final sample gave a spectrum identical to that of the *seco*-ZnPz.

Analysis

The absorption spectra, shown in parts a and j of Figure 2, are identical to those published previously and can be assigned to ZnPz and *seco*-ZnPz, respectively.[4] The presence of the isosbestic (isoabsorptive) points at 676, 630, 572, 553, 377, and 349 nm is indicative of a shift in equilibrium between two absorbing species with the total concentration remaining unchanged.[12] If the first (Figure 2a) and last spectra (Figure 2j) in this series are representative of the initial ZnPz and the *seco*-ZnPz, respectively, then all intermediate spectra will therefore be a linear combination of these two. The initial concentration and absorbance allow the molar decadic extinction coefficients of both species to be determined. Using the wavelengths of 648 and 596 nm, which represent the Q-band absorption maxima for the ZnPz and *seco*-ZnPz species, respectively, the concentration of the ZnPz and *seco*-ZnPz at different times can be determined. The absorbance at these two wavelengths is given by

TABLE 1: Molar Decadic Extinction Coefficients for ZnPz and *seco*-ZnPz at 596 and 648 nm Determined from the Spectra at $t = 0$ and $t = >70$ min with the Sample Concentration, $c = 1.07 \times 10^{-5}$

	ZnPz		*seco*-ZnPz	
wavelength/nm	A	ϵ/dm^{-3} mol^{-1} cm^{-1} (±50)	A	ϵ/dm^{-3} mol^{-1} cm^{-1} (±50)
596	0.323	30190	0.110	10280
648	0.194	18130	0.410	38320

$$A^{596} = c_{\mathrm{ZnPz}}\epsilon^{596}_{\mathrm{ZnPz}} + c_{seco-\mathrm{ZnPz}}\epsilon^{596}_{seco-\mathrm{ZnPz}}$$
$$A^{648} = c_{\mathrm{ZnPz}}\epsilon^{648}_{\mathrm{ZnPz}} + c_{seco-\mathrm{ZnPz}}\epsilon^{648}_{seco-\mathrm{ZnPz}} \quad (1)$$

where A = absorbance, c = concentration (mol dm^{-3}), and ϵ = molar decadic extinction coefficient (dm^3 mol^{-1} cm^{-1}). The wavelength and species are indicated as the superscript and subscript, respectively.

The four molar decadic extinction coefficients are given in Table 1. With these data the two simultaneous equations in eq 1 can be solved to give the relative concentrations of ZnPz and *seco*-ZnPz and these are plotted in Figure 7.

The functional form of these kinetic data is neither first nor second order, but is indicative of autocatalysis, where the product, *seco*-ZnPz, catalyzes the rate of photoperoxidation of the ZnPz. The rate law for the autocatalysis is given by

$$\mathrm{ZnPz} \xrightarrow{k} seco\text{-ZnPz} \quad (2)$$

where

$$\frac{-\mathrm{dZnPz}}{\mathrm{d}t} = k[\mathrm{ZnPz}][seco\text{-ZnPz}] = \frac{\mathrm{d}[seco\text{-ZnPz}]}{\mathrm{d}t} \quad (3)$$

The solutions of this scheme are:

$$[\mathrm{ZnPz}] = [\mathrm{ZnPz}]_0 - \frac{b[\mathrm{ZnPz}]_0(\exp^{at} - 1)}{1 + b\exp^{at}} \quad (4)$$

$$[seco\text{-ZnPz}] = [seco\text{-ZnPz}]_0 + \frac{b[\mathrm{ZnPz}]_0(\exp^{at} - 1)}{1 + b\exp^{at}} \quad (5)$$

where

$$a = ([\mathrm{ZnPz}]_0 + [seco\text{-ZnPz}]_0)k$$

and

$$b = \frac{[seco\text{-ZnPz}]_0}{[\mathrm{ZnPz}]_0}$$

k is an apparent second-order rate constant for the process (see below). With values of $[\mathrm{ZnPz}]_0 = 1.1 \times 10^{-5}$ mol dm^{-3}, [*seco*-

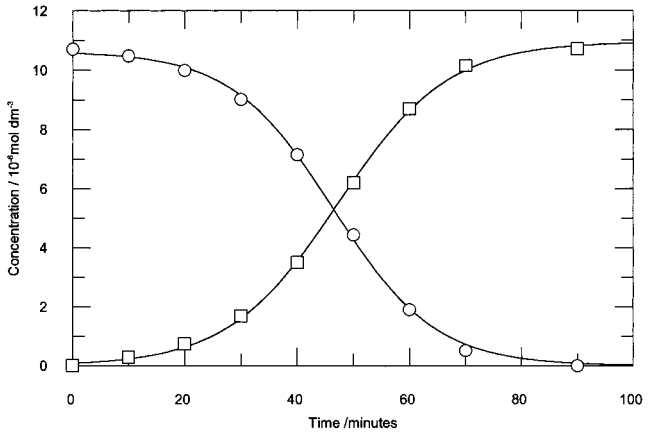

Figure 7. Concentration of ZnPz (diamonds) and *seco*-ZnPz (squares) as a function of irradiation time. The solid lines are a fit of the data using eqs 4 and 5 with $[ZnPz]_0 = 1.1 \times 10^{-5}$ mol dm^{-3}, $[seco\text{-}ZnPz]_0 = 7.0 \times 10^{-9}$ mol dm^{-3}, and $k = 1.5 \times 10^4$ dm^3 mol^{-1} min^{-1}.

$ZnPz]_0 = 7 \times 10^{-9}$ mol dm^{-3}, and $k = 1.5 \times 10^4$ dm^3 mol^{-1} min^{-1} the data were satisfactorily modeled using eqs 4 and 5, the results of which are shown as the solid lines in Figure 7.

Here, the oxidation is not caused by $^1O_2$ produced through sensitization by the reactant (suicide) but rather by $^1O_2$ produced through sensitization by the product (murder). The overall process can be summarized as follows:

$$^1seco\text{-ZnPz} + h\nu \rightarrow {}^1seco\text{-ZnPz}^* \qquad \text{absorption of a photon}$$

$$^1seco\text{-ZnPz}^* \rightarrow {}^3seco\text{-ZnPz}^* \qquad \text{intersystem crossing}$$

$$^3seco\text{-ZnPz}^* + {}^3O_2 \rightarrow {}^1seco\text{-ZnPz} + {}^1O_2$$
sensitized production of singlet oxygen

$$^1O_2 + ZnPz \rightarrow seco\text{-ZnPz} \qquad \text{peroxidation process}$$

To be consistent with the model, the concentration of singlet oxygen must be directly proportional to the concentration of *seco*-ZnPz such that the proportionality constant remains unchanged during the course of the reaction. These assumptions can be shown to be true (see appendix) if the following criteria are met.

(1) Some minimal sensitization must first occur in order to initiate the photoperoxidation, but the rate of this process is rapidly exceeded by the *seco*-ZnPz.

(2) The rate constant for the peroxidation process is very small with respect to the normal, unimolecular deactivation rate constants of the singlet oxygen.

(3) The concentration of dissolved oxygen must be large with respect to the initial concentration of ZnPz, such that it remains effectively unchanged during the course of the photoperoxidation. In this case, the apparent second-order rate constant is expected to be proportional to the light intensity and related to the ground-state oxygen concentration (see appendix).

The initial concentration of *seco*-ZnPz, $[seco\text{-}ZnPz]_0$, was determined to be 7×10^{-9} mol dm^{-3}, a value that is 3 orders of magnitude smaller than that of the ZnPz starting material. The experiment was repeated twice more with the starting solution spiked with different amounts of *seco*-ZnPz. In both cases, the overall rate of reaction increased dramatically, although the derived second-order rate constant, *k*, was found to have a value within 10% of the value for the unspiked reaction. It is thus evident that the sensitizing properties of the *seco*-ZnPz product far exceed those of the ZnPz starting material. This conclusion is consistent with the results from the triplet state studies in which the quantum yield for triplet state formation, ϕ_T, is 0.64 for the *seco*-ZnPz but immeasurable for the ZnPz. The rapid growth of the singlet oxygen signal, when examining air-equilibrated solutions of ZnPz, can similarly be attributed to the formation of *seco*-ZnPz which then catalyzes further production. The singlet oxygen phosphorescence signal decays at the same rate during the course of the photoperoxidation, which demonstrates that the rate constant for this chemical reaction is small with respect to the rate constants for the other excited-state deactivation mechanisms, as required by the second criterion listed above, for the autocatalysis kinetic mechanism. The final requirement, that the concentration of normal, triplet state oxygen remains unchanged, is also fulfilled as the initial concentration of ZnPz was 1.07×10^{-5} mol dm^{-3} while that of dissolved oxygen in toluene at room temperature[13] is 200 times higher at 2×10^{-3} mol dm^{-3}.

The photoperoxidation of ZnPz to *seco*-ZnPz results from the attack on ZnPz by singlet oxygen that is sensitized by the triplet state of the *seco*-ZnPz product (vide supra). The concentration of ground-state oxygen remains unchanged during the chemical reaction and the rate constant for the photoperoxidation process is much smaller than all other excited-state deactivation mechanisms for singlet oxygen. These effects lead to a concentration of the reactive, singlet oxygen that is proportional to the concentration of the product, *seco*-ZnPz (eq A5) and hence an autocatalytic kinetic mechanism is observed. The rate constant, *k*, is independent of the initial concentrations of both ZnPz and *seco*-ZnPz, although it does depend on the light intensity and on $[^3O_2]$, but this was not explored fully. Using the same irradiation conditions, the effect of solvent was very pronounced with noncoordinating solvents, such as toluene, cyclohexane, and dichloromethane behaving in a similar fashion. The use of pyridine as a coordinating solvent reduced the rate constant for the reaction by a factor of 20. This is consistent with our previous observation[4] that ZnPz appeared to be more stable in coordinating solvents.

Discussion

The photophysical data for ZnPz suggests that the dominant deactivation process for the first excited singlet state is neither fluorescence nor intersystem crossing and by the process of elimination it is probably direct internal conversion to the ground state, followed by vibrational relaxation. The *seco*-ZnPz is more interesting photophysically, exhibiting fluorescence as well as intersystem crossing ($\phi_T = 0.64$) as the dominant deactivation pathway. The sensitivity of fluorescence spectroscopy enables the radiative process to be observed readily even though it is 200 times less efficient. Again internal conversion probably constitutes the remaining 36% of the deactivation mechanisms. The emission peak at 605 nm we assign to a small amount of octapropyl zinc porphyrazine not observable by electronic absorption or other techniques. The emission at 708 nm from the *seco*-ZnPz has a very low fluorescence quantum yield. It decays biexponentially, but both of the measured fluorescence decay times are relatively long, results that are consistent with long natural, radiative lifetimes. As a guide, the average lifetime of the emission of 0.6 ns can be combined with quantum yield to produce a natural radiative lifetime of 170 ns. This value is inconsistent with the very large extinction coefficient ($\epsilon^{648} = 38\,320$) for the lowest energy Q-band of the *seco*-ZnPz, where the Strickler−Berg relationship[14] predicts a value closer to 2

ns. It could, however, be due to emission emanating from a state of the *seco*-ZnPz that is lower in energy than the Q-band at 648 nm, but is not coupled radiatively with the ground state and does not appear in the absorption spectrum. This argument is consistent with the large Stokes shift between the lowest energy absorption band (648 nm) and the emission maximum at 708 nm.

The production of singlet oxygen by *seco*-ZnPz must occur via the triplet state as the excited singlet state of *seco*-ZnPz is too short lived to interact with ground-state oxygen by diffusion. The quantum yield of singlet oxygen production is a combination of the intersystem crossing and sensitization by quenching. Since ZnPz has a low intersystem crossing quantum yield, the difficulty in measuring a singlet oxygen signal for ZnPz may not be due to inefficiency in the sensitization by the triplet state. The peroxidation process is, however, initiated. This may be an indication that sensitization by ZnPz is possible, but not easily measured, or that the process is initiated by the extremely small amount of octapropyl zinc porphyrazine that fluoresces at 605 nm. The efficiency of *seco*-ZnPz in promoting the sensitization is due to high yields of both intersystem crossing and quenching. The quantum yields for the two processes, $\phi_T = 0.64$ and $\phi_\Delta = 0.54$, respectively, indicate that quenching of the triplet state of *seco*-ZnPz by ground-state oxygen is indeed the major deactivation pathway. The high quantum yield of triplet state formation could be promoted by the two carbonyl groups on the *seco*-ZnPz, as this group is well-known to promote intersystem crossing.[15]

Conclusion

The photoperoxidation of ZnPz proceeds via the attack of $^1O_2$ on a peripheral pyrrole ring to produce *seco*-ZnPz. Once initiated, the reaction accelerates due to more efficient sensitization of the oxygen by the photoproduct, *seco*-ZnPz. As a consequence, the reaction proceeds autocatalytically with a second-order rate constant, the magnitude of which depends on the light intensity and on the concentration of dissolved oxygen. The photophysical characterization of the *seco*-ZnPz reveals a low fluorescence quantum yield and a high intersystem quantum yield. The triplet state lifetime is long ($\tau = 81\ \mu$s in the absence of oxygen), allowing for efficient interaction with dissolved $^3O_2$ to produce the active $^1O_2$, with a quantum yield of 0.54. This high value explains the efficiency of the photoperoxidation and also the autocatalytic mechanism. The use of coordinating solvents, such as DMF and pyridine, prevents the photooxidation process by inhibiting the efficiency of photosensitization by the *seco*-ZnPz. The photosensitized production of $^1O_2$ by *seco*-ZnPz is very efficient which would make this dye extremely phototoxic and confirms the overall photooxidation as murder and not suicide.

Acknowledgment. We thank Prof. David Phillips, the Glaxo Group Research Ltd. for the generous endowment (A.G.M.B.), the Wolfson Foundation for establishing the Wolfson Centre for Organic Chemistry in Medical Science at Imperial College, the Engineering and Physical Sciences Research Council, the National Science Foundation, and NATO for generous support of our studies.

Appendix

If it is assumed that the rate of photoperoxidation is slow with respect to the excited-state kinetics and that the process has been initiated (i.e., $[^1\text{seco}] \neq 0$) then the following rate equations can be written:

$^1\text{seco} + h\nu_a \rightarrow {}^1\text{seco}^*$	$k_a[^1\text{seco}][h\nu_a]$	absorption
$^1\text{seco}^* \rightarrow {}^1\text{seco} + h\nu_f$	$k_R^S[^1\text{seco}^*]$	fluorescence
$^1\text{seco}^* \rightarrow {}^3\text{seco}^*$	$k_{ISC}^S[^1\text{seco}^*]$	intersystem crossing
$^1\text{seco}^* \rightarrow {}^1\text{seco}$	$k_{IC}^S[^1\text{seco}^*]$	internal conversion
$^3\text{seco}^* \rightarrow {}^1\text{seco} + h\nu_p$	$k_R^T[^3\text{seco}^*]$	phosphorescence
$^3\text{seco}^* \rightarrow {}^1\text{seco}$	$k_{ISC}^T[^3\text{seco}^*]$	intersystem crossing
$^3\text{seco}^* + {}^3O_2 \rightarrow {}^1\text{seco} + {}^1O_2^*$	$k_Q^T[^3\text{seco}^*][^3O_2]$	sensitization
$^1O_2^* \rightarrow {}^3O_2 + h\nu_\Delta$	$k_R^\Delta[^1O_2^*]$	phosphorescence
$^1O_2^* \rightarrow {}^3O_2$	$k_{ISC}^\Delta[^1O_2^*]$	intersystem crossing

This quenching of the singlet state of *seco*-ZnPz by oxygen is assumed to be a minor deactivation pathway.

Writing rate equations and then using the steady-state approximation gives

$$\frac{d[^1O_2^*]}{dt} = k_Q^T[^3\text{seco}^*][^3O_2] - (k_R^\Delta + k_{ISC}^\Delta)[^1O_2^*] = 0 \qquad \text{(A1)}$$

$$\Rightarrow [^1O_2^*] = \frac{k_Q^T[^3\text{seco}^*][^3O_2]}{(k_R^\Delta + k_{ISC}^\Delta)}$$

$$\frac{d[^3\text{seco}^*]}{dt} = k_{ISC}^S[^1\text{seco}^*] - (k_Q^T[^3O_2] + k_R^T + k_{ISC}^T)[^3\text{seco}^*] = 0$$

$$\Rightarrow [^3\text{seco}^*] = \frac{k_{ISC}^S[^1\text{seco}^*]}{(k_Q^T[^3O_2] + k_R^T + k_{ISC}^T)} \qquad \text{(A2)}$$

$$\frac{d[^1\text{seco}^*]}{dt} = k_a[^1\text{seco}][h\nu_a] - (k_R^S + k_{ISC}^S + k_{IC}^S)[^1\text{seco}^*] = 0$$

$$\Rightarrow [^1\text{seco}^*] = \frac{k_a[^1\text{seco}][h\nu_a]}{(k_R^S + k_{ISC}^S + k_{IC}^S)} \qquad \text{(A3)}$$

Substituting equation A3 into A2 gives

$$[^3\text{seco}^*] = \frac{k^S{}_{ISC}}{(k_Q^T[^3O_2] + k_R^T + k_{ISC}^T)} \frac{k_a[^1\text{seco}][h\nu_a]}{(k_R^S + k_{ISC}^S + k_{IC}^S)} \qquad \text{(A4)}$$

Substituting equation A4 into A1 gives

$$[^1O_2^*] = \frac{k_Q^T[^3O_2]}{(k_R^\Delta + k_{ISC}^\Delta)} \frac{k_{ISC}^S}{(k_Q^T[^3O_2] + k_R^T + k_{ISC}^T)} \frac{k_a[h\nu_a][^1\text{seco}]}{(k_R^S + k_{ISC}^S + k_{IC}^S)} \qquad \text{(A5)}$$

The rate equation for the oxidation process, ZnPz + $^1O_2^* \xrightarrow{k_r}$ *seco*-ZnPz, is given by

$$\frac{d[^1\text{ZnPz}]}{dt} = -k_r[^1\text{ZnPz}][^1O_2^*] \qquad \text{(A6)}$$

Substituting for $[^1O_2^*]$ from A5 into A6 gives the experimentally observed relationship

$$\frac{d[^1\text{ZnPz}]}{dt} = -k[^1\text{ZnPz}][^1\text{seco}] \qquad \text{(A7)}$$

where the apparent second-order rate constant is defined by

$$k = k_r \frac{k_Q^T[^3O_2]}{(k_R^\Delta + k_{ISC}^\Delta)} \frac{k_{ISC}^S}{(k_Q^T[^3O_2] + k_R^T + k_{ISC}^T)} \frac{k_a[h\nu_a]}{(k_R^S + k_{ISC}^S + k_{IC}^S)} \quad \text{(A8)}$$

Thus, k is proportional to the light intensity, $[h\nu]$, and related to the oxygen concentration, $[^3O_2]$, unless $k_Q^T[^3O_2] \gg k_R^T + k_{ISC}^T$, when it becomes independent.

References and Notes

(1) Mani, N. S.; Beall, L. S.; Miller, T.; Anderson, O. P.; Hope, H.; Parkin, S. R.; Williams, D. J.; Barrett, A. G. M.; Hoffman, B. M. *J. Chem. Soc., Chem. Commun.* **1994**, 2095.

(2) Linstead, R. P.; Whalley, M. *J. Chem. Soc.* **1952**, 4839.

(3) Mani, N. S.; Beall, L. S.; White, A. J. P.; Williams, D. J.; Barrett, A. G. M.; Hoffman, B. M. *J. Chem. Soc., Chem. Commun.* **1994**, 1943.

(4) Garrido Montalban, A.; Lange, S. J.; Beall, L. S.; Mani, N. S.; Williams, D. J.; White, A. J. P.; Barrett, A. G. M.; Hoffman, B. M. *J. Org. Chem.* **1997**, *62*, 9284.

(5) Andersen, K.; Anderson, M.; Anderson, O. P.; Baum, S.; Baumann, T. F.; Beall, L. S.; Broderick, W. E.; Cook, A. S.; Eichhorn, D. M.; Goldberg, D.; Hope, H.; Jarrell, W.; Lange, S. J.; McCubbin, Q. J.; Mani, N. S.; Miller, T.; Garrido Montalban, A.; Rodriguez-Morgade, M. S.; Lee, S.; Nie, H.; Olmstead, M. M.; Sabat, M.; Sibert, J. W.; Stern, C.; White, A. J. P.; Williams, D. B. G.; Williams, D. J.; Barrett, A. G. M.; Hoffman, B. M. *J. Heterocycl. Chem.* **1998**, *35*, 1013.

(6) Bruckner, C.; Rettig, S. J.; Dolphin, D. *J. Org. Chem.* **1998**, *63*, 2094.

(7) Williams, A. J. R. *Analyst* **1983**, *108*, 1067.

(8) O'Connor, D. V.; Phillips, D. *Time-Correlated Single-Photon Counting*; Academic Press: London, 1983.

(9) Bensasson, R.; Goldschmidt, C. R.; Land E. J.; Truscott T. G. *Photochem. Photobiol.* **1978**, *28*, 277.

(10) Redmond, R. W.; Heihoff, K.; Braslavsky S. E.; Truscott T. G. *Photochem. Photobiol.* **1987**, *45*, 209.

(11) Wilkinson, F.; Helman, W. P.; Ross, A. B. *J. Phys. Chem. Ref. Data*, **1993**, *22* (1), 113.

(12) Cohen, M. D.; Fischer, E. *J. Chem. Soc.* **1962**, *3*, 3044.

(13) Murov, S. L.; Carmichael, I.; Hug, G. L. *Handbook of Photochemistry*, 2nd ed.; Marcel Dekker: New York, 1993; p 289.

(14) Ware, W. R.; Baldwin, B. A. *J. Chem. Phys.* **1963**, *40*, 1703.

(15) Gilbert, G.; Baggott, J. *Essentials of Molecular Photochemistry*; Blackwell: Cambridge, MA, 1991; p 126.